UNIVERSITY OF PARDUBICE

JAN PERNER TRANSPORT FACULTY


# FRACTURE TOUGHNESS ANALYSIS OF AUTOMOTIVE STEEL IN PLANE STRESS

Sunilkumar M R

A THESIS SUBMITTED FOR

THE DEGREE OF DOCTOR OF PHILOSOPHY

(ANNOTATION)

2021

**Programme of Study:** P3710 Technique and Technology in Transport and Communications
**Branch of Study:** 3706V005 Transport Means and Infrastructure
**Supervisor:** Prof. Ing. Eva Schmidová, Ph.D.
*Fracture toughness analysis of automotive steel in plane stress*
**The doctoral dissertation has arisen at the supervising:**
Educational and Research Centre in Transport.

## ABSTRACT

Determination of fracture toughness of the automotive steels in the plane stress dominant condition (thin sheets) using essential work of fracture methodology is the research work's objective. The lack of proper international standards and complicated testing methodology has forced us to search for an easy and reliable alternative method. Most of the existing international standards to measure fracture toughness are primarily designed based on plane strain dominant condition (thickness constraint). A comprehensive literature survey has been done on the essential work of fracture (EWF) method, and the parameters affecting it are studied. The essential work of fracture (EWF) methodology has been successfully used to determine the fracture toughness of dual-phase (DP450) steel and Interstitial free steel. The feasibility of the EWF methodology in mode-2 and mixed-mode is tested. The effect of notch tip radius on the fracture toughness in the EWF methodology is analysed. Using the EBSD analysis, comprehensively all material parameters affecting the fracture toughness are studied. Fractographic analyses of the fractured surfaces after the EWF test is done using a scanning electron microscope (SEM). Local strain during the essential work of fracture methodology has been studied for the DP450 and the IF steel. Forming limit diagrams (FLD) and fracture forming diagrams (FFD) are constructed for the DP450 and the IF steel. A hole expansion test is also done for the DP450 steel and the IF steel. Finally, a thorough comparison is made between all the parameters mentioned above.
***Keywords:*** Fracture toughness, EWF, Dual-phase steel, DP450, Interstitial free steel, Plane stress, FLD, Hole expansion ratio.

## TABLE OF CONTENTS

## 1. INTRODUCTION

Automotive manufacturing has been a significant contributor to the rapid economic growth of most countries on earth since the 19th century. A faster mode of transportation helps in moving goods and people from one place to another at a higher speed in comparison to traditional methods. Lack of infrastructure and automotive technology in developing and underdeveloped countries have failed to transport goods and people from one place to another place quickly, which led to slower economic progress. The automotive industry has made significant and progressive changes from the initial days, and it is a never-ending process. Today, the automotive industry is going through unprecedented changes such as electric vehicles, hybrid vehicles, autonomous driving, hydrogen fuel cell vehicles, and many more.

In the dawn of the automotive industry era, manufacturing a vehicle was a mammoth task, and vehicles were produced in small batches. Later, in the mass production assembly-line era, manufacturers' interest shifted towards speed, comfort, efficiency, reliability, quality, cost, robustness, etc. Today, extensive competition and strict norms from the government forced the automotive industry to produce more efficient and safer cars. The vehicle's weight has a significant effect on the vehicle's efficiency, and the safety of the cars is equally essential. Increased safety norms from the government and higher crash safety rating expectations from customers are constantly growing. Both efficiency and crash test performance of the vehicles are significantly dependent on the material used for vehicle manufacturing. To reduce gross weight and simultaneously to increase the strength of the vehicle, automakers have started to use advanced high strength steels (AHSS) in the last few decades. These advanced high-strength steels have higher strength than ordinary steel and have a significantly higher strength-to-weight ratio.

AHSS steels are expected to have good manufacturability, formability, weldability, corrosion resistance, durability, and cost-effectiveness. Ordinary low carbon steel has good ductile properties; however, it has relatively lower strength. Advanced high-strength steels are developed with different microstructural phases and alloying elements. Generally, these steels have very high yield strength and ultimate strength. Some of the advanced high strength steels used in the automotive industry are dual-phase (DP) steel, martensitic steel, complex steel, ferrite-bainitic steel, transformation induced plasticity (TRIP) steel, twinning induced plasticity steel, and many more. Generally, these steels have yield strength of more than 550 MPa (not a strict definition). Based on strength, fatigue, toughness, cost, and stiffness, these steels are used in various automotive components. Extensive research is needed on these steels in all areas to understand their mechanical properties entirely.

Fracture toughness parameters are critical for automotive steel. Fracture toughness has a direct influence on crashworthiness, formability, crack growth, and many more aspects. The majority of international Standards that measure fracture toughness are valid in plane strain conditions, i.e., for relatively thicker materials. A large portion of the automotive vehicle is made up of thin sheets. Determination of fracture toughness for thin sheets in-plane stress dominant condition is complicated, and there are no suitable and consistent international standards available.

Study and analysis of fracture toughness and microstructure of a few automotive steel sheets in plane stress dominant condition are among the primary focus of this research work. Dual-phase steel and interstitial free steel were chosen for the research work. These steels are extensively used in the automotive industry.

The essential work of fracture (EWF) method is used in this research work to find out fracture toughness of thin sheets in plane stress dominant condition. The EWF method and the parameters affecting it

will be analysed. Double edge notched tension (DENT) samples with fatigue pre-cracks are used. The EWF experiments are conducted in a universal tensile testing machine in assistance with ARAMIS digital image correlation (DIC) technique. The tested samples are analysed in an optical and electronic microscope for fractographic study. Electron backscatter diffraction (EBSD) analysis is done for the tested samples. Finally, fracture toughness of the dual-phase steel and the interstitial free steel are analysed, and their microstructural behaviours are studied using the EBSD analysis.

**Dual-phase (DP)** steel usage is constantly increasing in the automotive industry, and it is expected to grow higher in the future. Dual-phase steel has both ferrite and martensite phases; the ferrite phase gives ductility to the steel, while the martensite enhances the strength. The strength of dual-phase steel is ranging widely from 400 to 1200 MPa. Both high formability and strength are the main advantage of dual-phase steel; also, it has good strain hardening ability, dent resistance, impact resistance, and bake hardenability. Generally, DP steel strength increases with an increase in the volume fraction of the martensite. The size, shape, and distribution of the martensite significantly influence the dual-phase steel's mechanical properties. Grain refinement and solid solution strengthening of the ferrite phase also help improve the strength of the material. Coarser distribution of the martensite is detrimental to fracture resistance, and extreme hardness of the martensite can be reduced by post quench tempering[1].

**Interstitial free (IF)** steel is another important type of steel used in automobiles, mainly for the door, fenders, sunroof, tailgate, and interior floor. Extreme low content of carbon (<0.005 weight percentage) and nitrogen in interstitial free steel makes an ideal choice for deep drawing applications. Vacuum degassing technology helps in keeping the carbon content below 30 ppm. Titanium and niobium are

also added to form carbides and nitrides, further reducing the interstitial carbon and nitrogen atoms. IF steel yield strength is around 140 to 150 MPa, and ultimate strength of up to 280 MPa. The addition of solid solution strengthening elements such as manganese and silicon will significantly improve the strength of IF steel additionally up to 100 MPa but at the cost of formability. Cold-rolled and annealed sheets are widely used in the automotive industry. A strong texture {111}|| normal direction (ND) (γ-fibre) is desirable to get high formability and increase in carbon content or solid solution strengthening elements is detrimental to the {111}/{100} ratio (decreases). Along with the formation of carbides and nitrides, Niobium helps stabilize the formation of {111}|| normal direction crystallographic orientation of iron atoms[2].

## 2. OBJECTIVE AND AIM OF THE RESEARCH WORK

### Problem definition

Components used in automotive body-in-white are primarily hot or cold stamped steel. Ultra-high strength components are often hot-stamped, while components like the door, fender, roof, tailgate, etc., are often cold stamped. Cracks that appeared during stamping constitute a significant problem in sheet metals. Components with larger (visible) cracks are scrapped immediately; however, the microscopic cracks of length in orders of micrometers may grow in successive forming processes or in-service life. Forming limit diagrams (FLD) are used to set the limit for unstable plastic deformation during stamping. During stamping, the global failure of components by necking is identified using Forming limit curves (FLC) and simulation of stamping. However, **edge cracks formed in stamping are a local formability failure, which cannot be characterised by FLC.** The usage of advanced high-strength steel (AHSS) is constantly increasing in the automotive industry. The AHSS are more likely to be damaged by edge cracks than traditional

mild steel or interstitial free steel. As edge cracks are non-repairable and non-reversible, components with edge cracks are often scraped instead of rework. Higher importance is being given to the maintenance of stamping tools to avoid the edge cracks of AHSS. Material selection is critical in preventing edge cracks, as it has the most significant influence on the formation of edge cracks. Fracture toughness of the material is an important parameter, which helps in characterising the crack resistance ability of the material during stamping as well as service life. Material having lower fracture toughness is more susceptible to edge cracks. Fracture toughness of material will depend on microstructural parameters like phase, grain size, the orientation of crystallography, inclusions, alloying elements, work hardening, etc. **Determination of fracture toughness of the material in its original thickness is essential for material characterisation.** Standard fracture-toughness measurement tests have direct or indirect restrictions on thickness, while the thickness of the sheet metal is determined by rolling (fixed sheet metal thickness).

**Scope of the research work**

Fracture toughness is a vital property of material, which helps select better the material for stamping applications. International standards for the measurement of fracture toughness use parameters like stress intensity factor ($K_{IC}$), *J*-integral ($J_{IC}$), and crack tip opening displacement (CTOD), for the determination of fracture toughness. However, in all the standards, plain strain dominant condition (thicker sample) is utilised to avoid the effect of geometry and excessive plastic deformation. Determining the fracture resistance of a material in its original cross-section is essential and vital for material selection. Automotive outer body components are made up of thin sheets of thickness in orders of millimetres**. Fracture toughness of material in plane stress dominant condition (thin sheets) is an important parameter to be determined.** The fracture toughness of the material determines the material's ability to resist the formation of edge cracks

and avoid further growth during the service life. Several steels are used in the automotive outer body components based on the requirement, cost, manufacturability, corrosion resistance, weight, strength, and many more factors.

Advanced high-strength steels are replacing conventional steels to improve strength and reduce the weight of an automobile. A more simple and effective method is essential for the measurement of fracture toughness of sheet metals. International standards like ASTM, ISO, etc., are expensive, tedious, and inappropriate for thin sheets. B. Cotterell first proposed the essential work of fracture (EWF) technique, and J. K. Reddel is relatively simple, and samples are prepared in their original thickness. European Structural Integrity Society (ESIS) has accepted the method for testing polymers. A small volume of research has been done on the method, especially for metals.

Dual-phase steel and interstitial free steel are widely used in the automotive industry. While interstitial free steel is being used for a long-time, dual-phase steel usage is continuously increasing.

**Objective of the research work**

- Study and analysis of Essential Work of Fracture (EWF) methodology for automotive body thin sheet metals.
    - Theoretical study of the methodology and application on sheet metals.
- Determination of fracture toughness using essential work of fracture (EWF) methodology for automotive body steels like dual-phase steel and interstitial free steel.
    - DENT specimens prepared from laser cutting and Electrical discharge machining (EDM) are used to determine fracture toughness in plane stress prevailing conditions.

    - Utilization of digital image correlation (DIC) technique to determine the local and global strain distribution during the EWF tests.
    - Microstructure and fractographic analyses using SEM and EBSD.
    - Comparison of the fracture toughness between the interstitial free steel and the dual-phase steel.
    - Determination of fracture toughness in mode-2 and mixed-mode.
- Optimization of geometrical parameters for a simplified method of testing.
    - Parameters like the sample's geometry, sample preparation method, fatigue crack, etc., are optimised for better results.
    - The consequence of notch tip radius and fatigue crack on the results are studied.
- Construction of Forming limit diagrams based on necking as well as the fracture.
    - Fracture forming limit (FFL) lines constructed from the same EWF tested samples.

## 3. ESSENTIAL WORK OF FRACTURE

### Fracture toughness dependence on thickness

Most international standards that measure fracture toughness are designed on plane strain dominant conditions. The primary reason is the large plastic deformation near crack-tip in plane stress prevalent condition (thin sheets). In thin materials, the plastic zone's size near the crack tip is larger than the thickness of the material. The plain strain tri-axial stress condition is relatively minimal in the case of thin materials. In the case of thin materials, the proportion of slant fracture is much more significant. In thick sections, due to the larger tri-axial

stress zone, a significant portion of the triaxial stress state will come outside the plastic zone, except near the in-plane surfaces. This high tri-axial stress (in thick sections) will help in flat fracture and smaller shear lips near the surfaces.

**Essential Work of Fracture theory**

K.B. Broberg[3] introduced the concept of crack tip regions and explained the hypothesis of an autonomous end region near the crack tip. According to Broberg, using regular fracture mechanics theories based on stress and surface energy concepts, it is irrelevant to explain the crack tip autonomous region, leading to singularity. This small autonomous crack tip region is the material property, and the plastic region outside this autonomous zone is not a material property. The plastic deformation around the autonomous region is dependent on geometry and loading conditions.

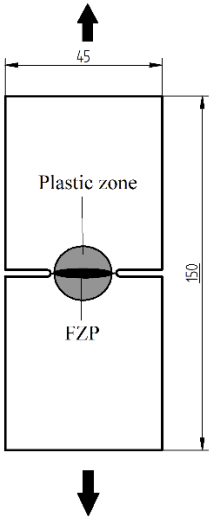


Figure 1. Schematic representation of fracture zones (mm).[4]

B. Cotterell and J. K. Reddel[5] extended Broberg's concept and proposed essential work of fracture concept (EWF). The authors divided the crack tip deformation zone into two separate zones, the

fracture process zone (FPZ) and the outer plastic deformation zone. The fracture process zone (FPZ) in ductile materials is independent of geometry or loading conditions, and it can be characterised as true material property.

In brittle materials, plastic deformation is minimal, and linear elastic fracture mechanics theories are enough to characterise the fracture behaviour. Generally, ductile materials have sizeable plastic deformation, and energy consumption increases as the crack grow. In plane strain prevailing conditions, the amount of energy distributed to the fracture process zone and the plastic deformation zone is almost constant throughout the crack growth. However, in the case of plane stress dominant loading condition, energy distributed for the plastic deformation is constantly increasing as the crack grows. As the crack extends, a more considerable portion of the energy is spent on the plastic deformation, while the amount of energy consumed in the fracture process zone is constant. This rising energy consumption for the plastic deformation will make linear elastic fracture mechanics inappropriate for thin sheets. Figure 1 shows the schematic representation of a Double Edge Notched Tension (DENT) specimen with FPZ and outer plastic deformation zone.

In the EWF method, the total energy absorbed by a specimen to fully fracture the specimen is taken as an input measurement. The energy consumed by the specimen is calculated by the area under the load-displacement curve and is given by

$$W_f = \int_0^{V_f} P dv \tag{3.1}$$

$W_f$ is the total energy consumed by the specimen to break completely, $v_f$ is the displacement at fracture, and $P$ is the load. This total energy is divided into two parts, the first part is the energy consumed by the fracture process zone (FPZ) near the crack tip ($W_e$), and the second part is the energy consumed for the plastic deformation around the crack tip ($W_P$).

$$W_f = W_e + W_P \quad (3.2)$$

These energies are called essential energy and non-essential energy, respectively. The essential energy is the energy consumed by the fracture process zone, and it is proportional to the ligament area. The non-essential energy is the energy consumed by the outer plastic deformation, which is a function of volume.

$$W_f = w_e L t + w_p L^2 t \beta \quad (3.3)$$

Where $w_e$ is specific essential work of fracture, $w_p$ is specific non-essential work of fracture, $L$ is the ligament length, $t$ is the thickness of the sheet, and $\beta$ is the plastic zone shape factor. The plastic zone shape factor is $\pi a/4b$, where $a$ and $b$ are the major axis and minor axis of the ellipse. For a circular shaped plastic zone, $\beta$ will become $\pi/4$. If the whole equation (Eq. 3.3) is divided by the area of the ligament. Then,

$$w_f = \frac{W_f}{Lt} = w_e + w_p L \beta \quad (3.4)$$

Where $w_f$ is specific work of fracture, it is a linear function of the ligament length with a slope of $w_p\beta$. Testing samples of different ligament lengths can calculate the value of $w_e$. Plot the results of $w_f$ versus the ligament length $L$, and then $w_e$ will be the intersection at zero ligament length. The $w_f$ values are extrapolated to zero ligament length using a linear regression curve. Specific essential work of fracture is constant for a material thickness. Generally, specific essential work of fracture increases with an increase in thickness[6]. Some basic requirements must be met during the experiments to validate the essential work of fracture methodology. The ligament should be fully yielded before the crack growth begins, and the ligament must be in a state of plane stress dominant condition. The crack growth before the complete yielding of the specimen leads to a contradiction of the methodology's fundamental principle. To keep the ligament in plane stress condition, the lower ligament length should be higher than three times the sample's thickness. The sample's upper

ligament is restricted to less than one-third of the total sample width or Irwin's second-order plastic zone. The upper limit is to avoid the formation of two individual plastic zones. Inside the ligament, quasi-plane strain condition will prevail at the crack beginning on either end. Equation 3.5 depicts the ligament length limits of the DENT sample for the EWF test. The lower limit of the ligament length is governed by quasi plane strain conditions, while the upper limit is restricted by forming two independent plastic zone.

$$3t \sim 5t < L < \frac{W}{3} \tag{3.5}$$

Elongation at fracture $v_f$ is a linear function of the length of the ligament and is defined as follows,

$$v_f = \delta_c^e + \frac{\psi^e}{2} L \tag{3.6}$$

Where $v_f$is the extension of the specimen at fracture, $\delta_c^e$is experimentally determined crack tip opening displacement, $\psi^e$is experimentally determined crack tip opening angle, and $L$ is ligament length. Theoretical background and related experiments of EWF methodology are found in the literature[7–14].

## 4. MATERIALS AND METHODOLOGY

### Materials

Chemical composition of DP450 and IF steels used in this research work is given in Table 1. The DP450 steel has a carbon percentage of 0.083 weight %, which helps formation of the martensite, manganese helps in stabilizing the austenite and strengthening of the ferrite. A good weldability is expected due to the low carbon content. A relative high portion of the manganese helps in grain refinement also[15]. Silicon helps for the transformation of the ferrite, and chromium helps to avoid the formation of bainite or pearlite during quenching. In the IF steel, as expected, shallow carbon and nitrogen contents are present and low strength is attributed to the absence of solute elements and secondary hard phases.

Table 1. Chemical composition of DP450 and IF steels in weight percentage.

| Sample | C | Mn | Si | P | S | Cr | Ni | Cu | Al | Ti | Fe |
|---|---|---|---|---|---|---|---|---|---|---|---|
| **DP450** | 0.083 | 1.72 | 0.026 | 0.021 | 0.0049 | 0.209 | 0.0097 | 0.014 | 0.056 | 0.163 | ~97 |
| **IF steel** | 0.018 | 0.110 | 0.024 | 0.0062 | 0.0076 | 0.033 | 0.036 | 0.026 | 0.051 | 0.056 | 99.58 |

Table 2 shows the mechanical properties determined from the standard tensile test for the DP 450 and IF steels.

Table 2. Mechanical properties of IF steel from the standard tensile test.

| | Angle to RD | $\sigma_y$(MPa) | $\sigma_u$(MPa) | $A_g$% | $A_{50}$% | $n$ | $r_p$ |
|---|---|---|---|---|---|---|---|
| **DP450** | 0º | 308 | 499 | 19.46 | 30.48 | 0.18 | 0.83 |
| | | 299 | 499 | 19.69 | 29.28 | 0.19 | 0.67 |
| | 45º | 262 | 504 | 19.03 | 26.68 | 0.18 | 0.52 |
| | | 327 | 502 | 16.67 | 20.81 | 0.17 | 0.66 |
| | 90º | 308 | 499 | 18.62 | 27.06 | 0.18 | 0.47 |
| | | 309 | 499 | 18.95 | 30.07 | 0.18 | 0.68 |
| **IF Steel** | 0º | 168 | 290 | 26.76 | 46.85 | 0.24 | 1.44 |
| | | 157 | 286 | 26.19 | 47.24 | 0.24 | 1.44 |
| | 45º | 165 | 281 | 25.24 | 47.65 | 0.20 | 1.43 |
| | | 160 | 282 | 26.28 | 45.68 | 0.21 | 1.34 |
| | 90º | 187 | 285 | 24.38 | 41.94 | 0.21 | 1.74 |
| | | 166 | 281 | 24.87 | 44.37 | 0.23 | 1.93 |

## EWF test

Essential work of fracture (EWF) methodology has been used to find out the fracture toughness of the DP450 and IF steel sheets. Double edge notched tension (DENT) specimens prepared from laser cutting and EDM technology are used for the EWF test. Figure 2 shows the DENT specimen with magnified notch-tip dimensions prepared from the laser and EDM cutting. In the EWF test, the sample is loaded in a universal tensile testing machine and pulled uniformly until the final fracture. Gauge length is difficult to identify in the DENT specimens;

hence, crosshead speed is considered a reference rather than strain rate. A constant crosshead speed of 1 mm/minute is used in all the EWF tests. The area under the load-displacement curve is the output of the test. An inbuilt load transducer and an extensometer respectively record the force and the displacement. The stress across the ligament in the EWF test is tensile; hence, no anti-buckling supports are needed. Grips on either end of the DENT specimen is free of speckle pattern for better gripping. A gripping length of approximately 25 mm is used in all the samples.

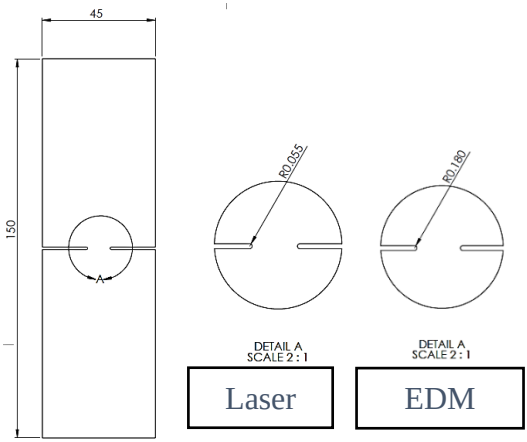


Figure 2. DENT specimen with magnified notch-tip dimensions prepared from laser and EDM cutting.

**Digital image correlation and hole expansion test**

Generally, strain and displacement obtained during the essential work of fracture (EWF) testing from an extensometer or a crosshead have only global data. Information obtained from the extensometer is the sample's average deformation without considering the local deformation. Digital image correlation (DIC) is a non-contact optical measurement technique, which utilizes a series of images and computation to give exact deformation at every location on a sample

Figure 3 shows a simple schematic representation of a **hole expansion test**. The essential components of the test are holders to hold a sample, cylindrical punch, and sample. An initial bore diameter ($d_o$) of the sample is selected as 35 mm. The cylindrical punch is moved into the bore until a fracture appears. The final diameter of the bore ($d_f$) is measured after the test. Several samples with different shearing clearance are prepared and tested. The hole expansion ratio $\lambda$ is calculated using equation 4.1. (Hole expansion test for the DP450 and the IF steel is done in the *Technical University of Liberec* in association with *Skoda auto*).

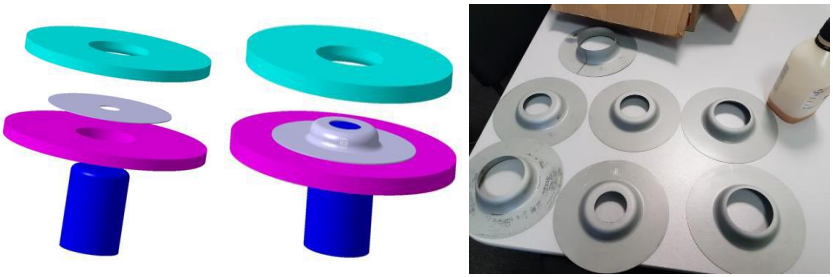

(a)

(b)

Figure 3. Schematic representation of hole expansion test[16]; (b) samples after the test.

$$\lambda = \frac{d_f - d_o}{d_o} \times 100 \qquad \text{Eq. (4.1)}$$

## 5. RESULTS AND DISCUSSIONS OF EWF TESTS

### DP450 steel

Figure 7 shows the force-deformation (displacement) curves for the notched samples prepared from the laser. From the visual observation and DIC images, crack initiation happens near the peak load for the notched samples. After the crack initiation, the decrease in load is not instantaneous; instead, it is more gradual. The gradual decrease in load indicates good crack growth resistance and ductile fracture during the crack growth.

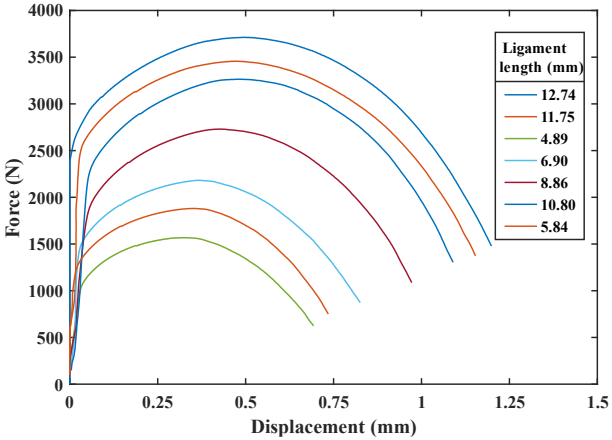


Figure 4. Force versus displacement diagram for notched samples prepared from the laser.

Table 3 shows the outputs and calculated parameters from the force-displacement curves of the EWF tests for the notched samples prepared from the laser. Figure 6 shows specific work of fracture versus ligament length for the notched samples prepared from the laser. The specific essential work of fracture *'$w_e$'* and slope of the fitted curve are 200.14±4.84 kJ/m$^2$ and 26.16±0.523 kJ/m$^3$respectively. An $R^2$ value of 0.9980 (Figure 6) indicates the fitted curve's good linearity. Figure 5 shows the graph of deformation at fracture versus ligament length for notched samples prepared from the laser. The determined

CTOD $\delta_c^e$ and CTOA $\psi^e$ from the EWF tests are 0.3625±0.0016 mm and 7.66º respectively. The fitted line has an $R^2$ value of 0.9962.

Table 3. EWF test outputs for notched samples prepared from the laser.

| Ligament length (mm) | Maximum force (N) | Maximum stress(MPa) | Total work of fracture $W_f$(N-mm) | $w_f$ (kJ/m$^2$) | $v_f$ (mm) |
|---|---|---|---|---|---|
| 4.89 | 1567.96 | 567.52 | 897.61 | 324.89 | 0.6933 |
| 5.84 | 1881.69 | 570.28 | 1161.41 | 351.99 | 0.7350 |
| 6.9 | 2182.24 | 559.76 | 1486.70 | 381.35 | 0.8258 |
| 8.86 | 2731.15 | 545.59 | 2194.78 | 438.44 | 0.9723 |
| 10.8 | 3264.99 | 535.07 | 2955.26 | 484.31 | 1.0896 |
| 11.75 | 3457.26 | 520.77 | 3370.35 | 507.68 | 1.1535 |
| 12.74 | 3713.00 | 515.83 | 3807.55 | 528.97 | 1.1988 |

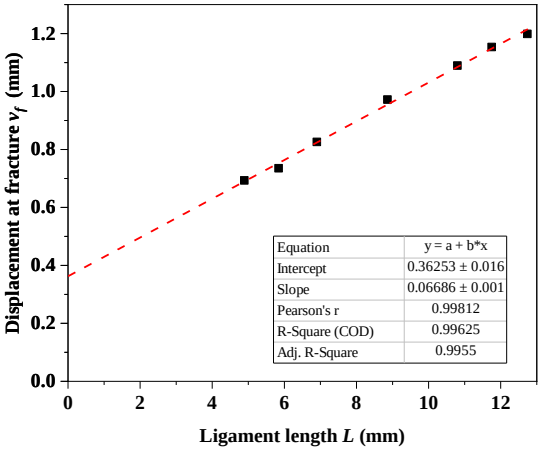


Figure 5. Deformation at fracture versus ligament length for notched samples prepared from the laser.

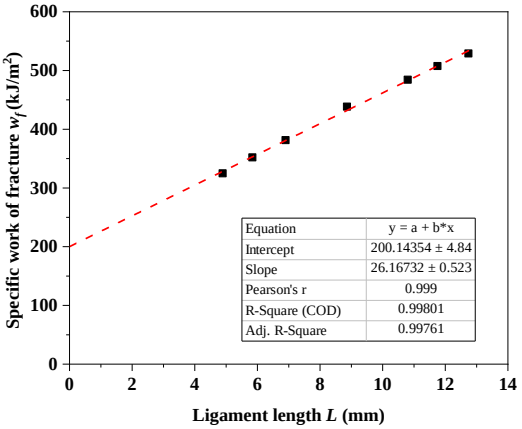


Figure 6. Specific work of fracture versus ligament length for notched samples prepared from the laser.

Figure 7 show the force-deformation (displacement) curves for the pre-cracked samples.

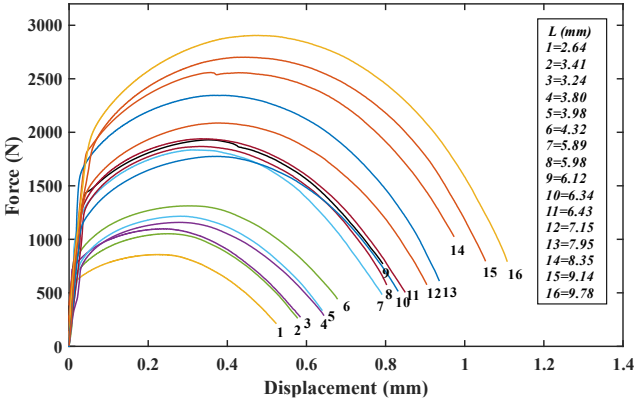


Figure 7. Force versus displacement diagram for precracked samples.

Figure 9 shows specific work of fracture versus ligament length for the precracked samples, and deformation is recorded from the extensometer. The specific essential work of fracture *'$w_e$'* and slope of the fitted curve are 154.22±7.26 kJ/m$^2$ and 32.34±1.15 kJ/m$^3$, respectively, which are significantly lower compared to the notched samples. An $R^2$ value of 0.9824 (Figure 9) indicates the fitted curve's

decent linearity. Figure 8 shows the graph of deformation at fracture versus ligament length for the precracked samples, and deformation is recorded from the extensometer. The determined CTOD $\delta_c^e$ and CTOA $\psi^e$ from EWF tests are 0.3251±0.01mm and 9.07º respectively. The fitted line has an $R^2$ value of 0.9917.

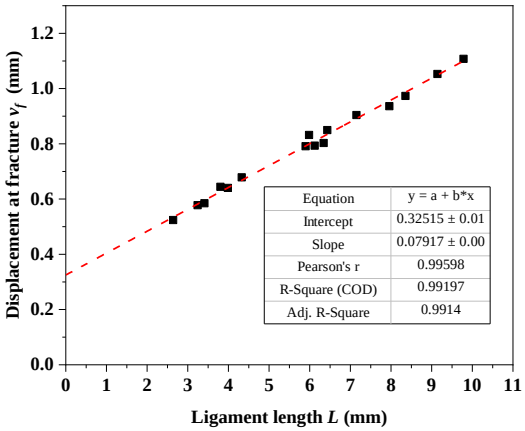


Figure 8. Deformation at fracture versus ligament length for precracked samples.

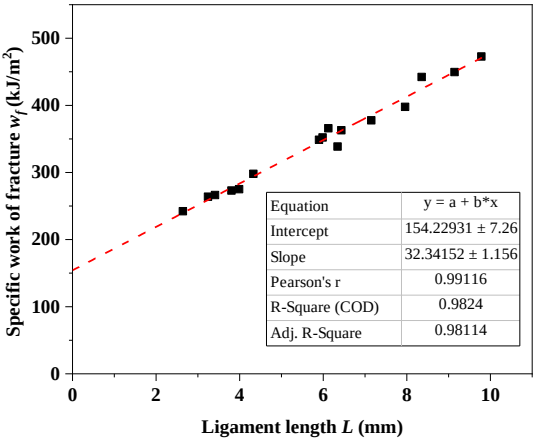


Figure 9. Specific work of fracture versus ligament length for precracked samples.

## IF steel

Table 4 tabulates the EWF test results for the notched and the precracked samples of the IF steel. The principal output of the EWF

test is specific essential work of fracture $w_e$, which doesn't decrease significantly for the precracked samples compared to the notched samples. The specific essential work of fracture $w_e$ for the notched samples is 8.39% larger than the precracked samples. Crack tip opening displacement $\delta_c^e$ for the notched samples is 17.93% larger than the precracked samples. Specific non-essential work of fracture $w_p$ ($w_p\beta$) is higher for the precracked samples, i.e., the curve slope (specific work of fracture vs. ligament length) is higher for the precracked samples. Crack tip opening displacement $\delta_c^e$ is more sensitive than $w_e$ to fatigue precrack. The crack tip opening angle $\psi^e$ and the specific non-essential work of fracture *'$w_p$'* have an opposite effect on the presence of fatigue precrack. Both the parameters are higher for the fatigue precracked samples compared to the notched samples. The vital information is both the parameters($\psi^e$ & $w_p$) are determined from the slope. while $w_e$ and $\delta_c^e$ are determined from zero intercepts.

Table 4. EWF test results for notched and precracked samples of **IF** steel.

| | $w_f = w_e + w_p L\beta$ | | | $v_f = \delta_c^e + \frac{\psi^e}{2} L$ | | |
|---|---|---|---|---|---|---|
| **Type** | **$w_e$ (kJ/m$^2$)** | **$w_p\beta$ (kJ/ m$^3$)** | **$R^2$** | **$\delta_c^e$(mm)** | **$\psi^e/2$ ($\psi^e$in $\theta^\circ$)** | **$R^2$** |
| **Notched** | 212.63 | 44.17 | 0.9969 | 0.5024 | 0.1559 (17.76º) | 0.9985 |
| **pre-cracked** | 196.16 | 52.42 | 0.9933 | 0.426 | 0.1724 (19.76º) | 0.9946 |

**Comparison of EWF results between DP450 and IF steel**

Essential work of fracture (EWF) methodology has been successfully used to calculate the fracture toughness of the Dual-phase (DP450) steel and the Interstitial free(IF) steel. These two sheets of steel have a different microstructure and mechanical properties. Both

the sheets of steel have been tested in notched and precracked conditions. For comparison of notched samples, samples prepared using the laser are chosen. Table 5 shows the detailed comparison of the DP450 steel and the IF steel EWF test results.

Table 5. EWF test results for notched and precracked samples of **DP450** and **IF steel.**

| Type | Material | $w_f = w_e + w_p L\beta$ | | | $v_f = \delta_c^e + \frac{\psi^e}{2} L$ | | |
|---|---|---|---|---|---|---|---|
| | | $w_e$ (kJ/m$^2$) | $w_p\beta$ (kJ/m$^3$) | $R^2$ | $\delta_c^e$(mm) | $\psi^e/2$ ($\psi^e$ in $\theta^\circ$) | $R^2$ |
| Notched | DP 450 | 200.14 | 26.16 | 0.9980 | 0.3625 | 0.06686 (7.66$^o$) | 0.9962 |
| | IF steel | 212.63 | 44.17 | 0.9969 | 0.5024 | 0.1559 (17.86$^o$) | 0.9985 |
| pre-cracked | DP 450 | 154.22 | 32.34 | 0.9824 | 0.325 | 0.079117 (9.07$^o$) | 0.9917 |
| | IF steel | 196.16 | 52.42 | 0.9933 | 0.4260 | 0.172 (19.76$^o$) | 0.9946 |

For the notched samples, the DP450 and the IF steels have $w_e$ values of 200.14 kJ/m$^2$ and 212.63 kJ/m$^2$, respectively. The IF steel has about 6% higher $w_e$ value than the DP450 steel. For the precracked samples, the DP450 and the IF steels have $w_e$ values of 154.22 kJ/m$^2$ and 196.16 kJ/m$^2$, respectively. The IF steel has about **27%** higher $w_e$ value than the DP450 steel. $w_e$ for both the steels are approximately similar for the notched samples. However, $w_e$ for the precracked samples have a significant difference. The presence of fatigue precrack in the DP450 steel has reduced $w_e$ by about 23%, while only 8% for the IF steel. Crack tip opening displacement $\delta_c^e$ for the DP450 and the IF steel are 0.3625 and 0.5024 mm, respectively, for notched samples. IF steel has about **39%** higher $\delta_c^e$ value than the DP450 steel for the notched

samples. Crack tip-opening displacement $\delta_c^e$ for the DP450 and the IF steel are 0.3251 and 0.4260 mm, respectively, for the precracked samples. For the precracked samples, the IF steel has about **31%** higher $\delta_c^e$ value than the DP450 steel. The presence of fatigue precrack in the DP450 steel has reduced $\delta_c^e$ by about 10%, while it is 15% for the IF steel. Specific non-essential work of fracture $w_p$ ($w_p\beta$) for the DP450 and the IF steel are 26.16 kJ/m$^3$ and 44.17 kJ/m$^3$, respectively, for the notched samples. For the precracked samples, $w_p$ ($w_p\beta$) for the DP450 and the IF steel are 32.34 kJ/m$^3$ and 52.42 kJ/m$^3$, respectively. Crack tip opening angle $\psi^e$ for the DP450 and the IF steel are 7.66º and 17.86º, respectively, for the notched samples. For the precracked samples, $\psi^e$ for the DP450 and the IF steel are 9.07º and 19.76º, respectively.

Specific essential work of fracture $w_e$ is sensitive to the notch tip radius; however, the sensitivity may vary from material to material. Both the DP450 and the IF steel have shown lower $w_e$ value for the precracked samples. However, the IF steel is less sensitive to the notch tip radius than the DP450 steel**.** Based on $w_e$ value, the IF steel's fracture toughness is higher than the DP450 steel by 27%. Crack tip opening displacement $\delta_c^e$ is also sensitive to the notch tip radius and has lower values for the precracked samples. Unlike $w_e$, $\delta_c^e$ is more sensitive to the notch tip radius for the IF steel. Based on $\delta_c^e$ value, fracture toughness of the IF steel is higher than the DP450 steel by 31%**.** From the comparison of both the parameters ($w_e$ & $\delta_c^e$) for the DP450 and the IF steel, the IF steel has higher fracture toughness than the DP450 steel.

Specific non-essential work of fracture $w_p$ ($w_p\beta$) is the curve slope in the graph of specific work of fracture versus ligament length. For both the notched and the precracked samples, the IF steel has a higher slope ($w_p\beta$) than the DP450 steel. In the graph of specific work of fracture

$w_f$ versus ligament length $L$, specific essential work of fracture $w_e$ is constant for all ligaments, and specific non-essential work of fracture $w_p$ ($w_p\beta$) increases with an increase in ligament length. A higher slope indicates more energy (specific non-essential work of fracture $w_p$) consumed as ligament length increases. From the above results, the IF steel consumes a higher amount of the non-essential work of fracture energy (plastic work) as ligament length increases. In comparison, the DP450 steel's rate of the non-essential work of fracture energy (plastic work) consumption with ligament length is lower than the IF steel. The primary reason for the above difference might be the IF steel's ability to redistribute the stresses away from the ligament. The non-essential work is dependent on geometry and loading conditions; however, both the materials are tested in identical conditions, so it is fair to compare. Crack tip opening angle $\psi^e$ is determined using slope from the graph of total elongation at fracture versus ligament length. For both the notched and the precracked samples, the IF steel has a higher $\psi^e$ than the DP450 steel, in general, the IF steel has larger deformation at fracture for every successive ligament length.

## 6. MICROSTRUCTURAL AND FRACTOGRAPHIC EVALUATION

EBSD scanning is done for as received steels and deformed steels from the EWF test. The EBSD scanning is done on an area of 118×88 µm, resolution of 512×384 pixels, exposure time of 16.4 milliseconds, accelerating current of beam 20 kV, probe current of ~20 nA, step size of 0.23 µm/pixel and 60.2 fps. The average grain sizes are 6.31 µm and 7.23 µm (from two analyses and without considering grains smaller than 100 pixels

Crystallographic orientation data obtained during EBSD scanning helps in identifying the texture of grains. Inverse pole figure (IPF) map uses basic colours to assign the crystal lattice orientation at every pixel

with respect to anyone's standard direction. For cubic crystals, each family of planes {111},{110} and {100} are assigned with a single colour. Figure 10(a) shows the inverse pole figure (IPF) maps in the z-direction for DP450 steel. There is no single orientation texture seen from the figure; however, a considerable amount of γ-fiber({111}||ND) in the normal direction is visible. The crystallographic orientation along {100} in the normal direction is detrimental for formability; a small number of grains are oriented in the {100}||ND direction. The lower ratio of {111}/{100} is an indication of poor formability. Upon deformation, the crystal lattice oriented close to {111}||ND rotated towards stable {111} and H.N. Han et al.[17] reported similar behaviour for DP steel after equi-biaxial tension. Also, the crystal lattice along {110} in the transverse direction becomes more intense.

Figure 10(b) shows the inverse pole figure(IPF) maps in the z-direction for IF steel. The initial crystallographic orientation of as-received IF steel has a strong γ-fiber ({111}||ND) and a partial α-fiber {110}||RD. Recrystallization after cold rolling helped in achieving a uniform crystallographic orientation. A favourable {111} crystallographic orientation in the normal direction helps excellent plastic deformation without strain localization. Some researchers have reported that upon cold rolling γ-fiber {111}||ND and partial α-fiber {110}||RD increase in IF steel[18,19]. After plastic deformation (EWF test), the γ-fiber {111}||ND and the α-fiber {110}||RD are increased. The crystallographic texture along {100} in the normal direction is present in small traces. A higher ratio of texture {111}/{100} is good for formability. Some researchers have reported an increase in γ-fiber upon plastic deformation[17], and a similar effect is also seen here. Francisco C.G. et al.[20] reported that γ-fiber({111}||ND) grains have

more internal misorientation than α-fiber {110}||RD grains after plastic deformation.

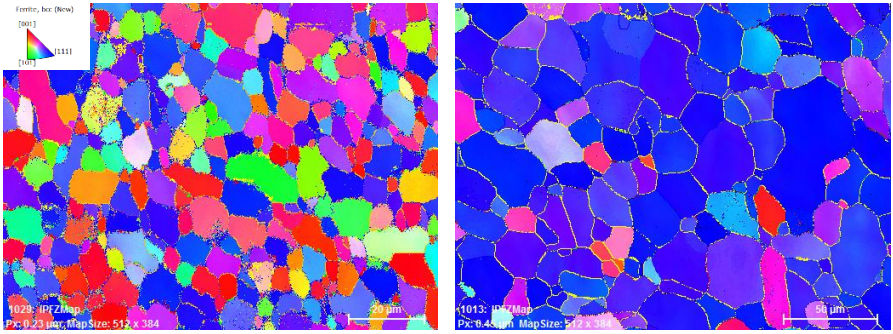

Figure 10. Inverse pole figure (IPF) map in normal direction: (a) DP450 steel; (b) IF steel.

**Fractographic evaluation**

The primary mode void generation in the DP450 steel is by ferrite-martensite decohesion. The difference in plastic strain compatibility between the two phases is the primary reason for decohesion[21]. No martensite cracking or severe deformation has been observed in the micrographs of the necking region. Martensitic cracking is a result of the extreme hardness of the martensite phase, which induces high stress on the martensite and severe strain on ferrite. The ferrite-ferrite decohesion is very rare and appeared only in proximity to martensite. Voids that appeared along the ferrite-ferrite grain boundary between closely situated martensite have grown longer. Figure 11 shows SEM micrographs of the DP450 and IF steels necking region after the EWF test. Voids formed only at the grain boundary interactions and appeared only close to the fracture surfaces. In the EBSD analysis of the homogeneously deformed portion (away from necking), there were no slip bands, and orientation within the grain is without any abrupt change in orientation. However, in the necking region, during severe plastic deformation close to the fracture surface, slip bands are formed about 45º to the loading axis.

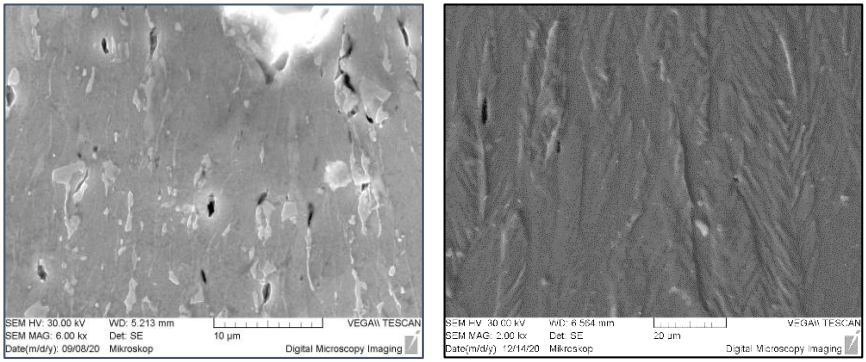


(a) (b)

Figure 11. Voids formation in necking region: (a) DP450 steel; (b) IF steel.

Figure 12 shows the fractured surface at the crack tip for the DP450 and IF steel. Ductile fracture prevails, which means that micro void nucleation and coalescence happened before the crack opening. At the crack tip, the stress state is quasi-plane strain and changes to the plane-stress dominant condition as the crack propagates. Unlike the DP450 steel, the necking intensity is very high in the IF steel. In both the conditions (notched and precracked), ductile fracture prevails, and the morphology of the cracked surface is similar. The absence of the transitional distance in the IF steel can be attributed to high plastic fracture strain.

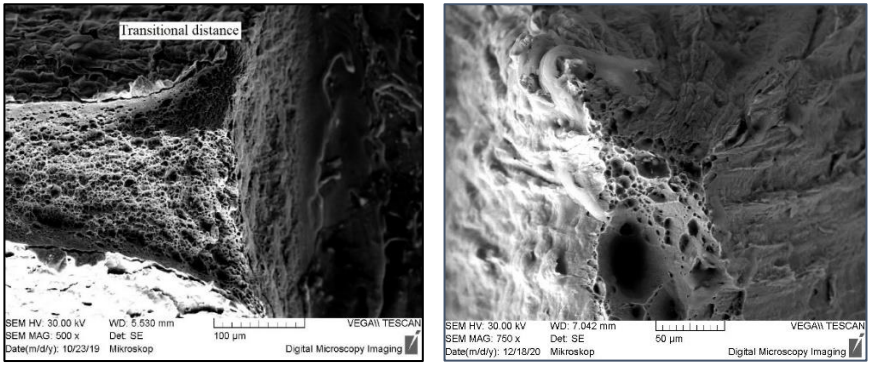


(a) (b)

Figure 12. Fractured surface at the crack tip: (a) DP450 steel; (b) IF steel.

## 7. STRAIN ANALYSES DURING EWF TEST

Figure 13 shows the Mises strain development at various stages during the EWF test for the DP450 steel. From the visual observation, plastic deformation is limited only to the ligament area, and the rest of the sample has no significant plastic deformation. The shape of the plastic zone around the ligament is slightly elliptical. The amount of deformation (strain) within the elliptical plastic zone around the ligament is not uniform. The area around the immediate vicinity of the ligament is called the necking zone and experienced severe deformation. The local strain inside the necking zone is significantly higher than the outer plastic zone. During the EWF test, after complete yielding, strains near notches are higher than the rest of the ligament. Half dumbbell-shaped strain patterns are created near the notches and intersect during crack propagation. The half dumbbell-shaped strain has a gradient strain pattern, and the strain decreases as it moves away from the notch centre. Stable crack growth happens only after reaching the maximum force. After the maximum force, strain outside the necking zone will not change significantly. The shape of the plastic zone and behaviour of strain is similar for both notched and precracked samples.

Figure 14 shows the Mises strain development at various stages during the EWF test for the IF steel. Like the DP450 steel, plastic deformation is limited to the ligament area, and the rest of the sample is largely unaffected. However, the spread of plasticity is much wider. The shape of the plastic deformation is slightly different in comparison to the DP450 steel. The shape of plastic deformation in the IF steel is also elliptical; however, the major axis (ellipse) is along the loading direction. During the initial loading stages, the shape of the plastic zone around the ligament is more circular. The high strain zone (more than 10%) is much wider for the IF steel than the DP450 steel. The

strain gradient rings at the notches are more circular and stretched outside the fracture zone (compared to the DP450).

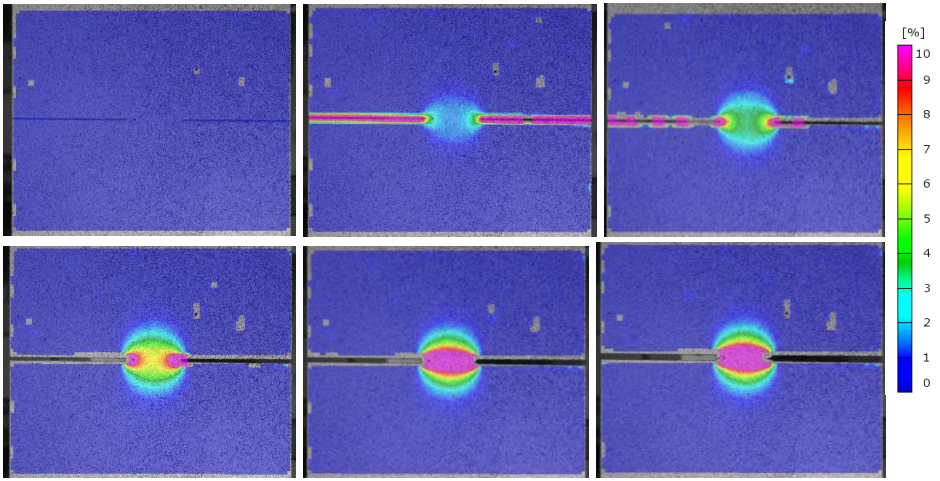


Figure 13. Mises strain development during the EWF test at various stages for DP450 steel.

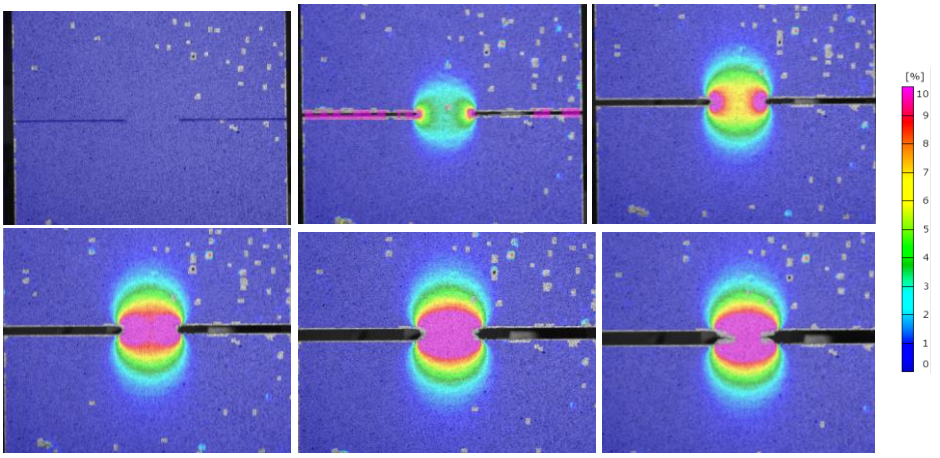


Figure 14. Mises strain development during EWF test at various stages for IF steel.

**Hole expansion test**

Table 6 and Table 7 show the hole expansion test results for the DP450 and IF steels. The original diameter of the hole is 35 mm for both the

steels. Cutting clearance is the gap between punch and die; it is also expressed in the sheet thickness percentage. The hole expansion ratio of the IF steel is significantly higher than the DP450 steel. At zero clearance, the hole expansion ratio of the DP450 and IF steels are 63.14 and 185.57 percentages respectively. The hole expansion ratio of the IF steel is about three times higher than the DP450 steel. With a maximum clearance of 0.4 mm, the hole expansion ratio of the DP450 and IF steels are 9.96 and 63.75 percentages respectively. The hole expansion ratio of the IF steel is about six times higher than that of the DP450 steel.

Table 6. Hole expansion test results of DP450 steel.

| **Final average diameter $d_f$ (mm)** | **Hole expansion ratio $\lambda$ (%)** | **Cutting clearance $C$ (mm)** | **Cutting clearance in % of thickness $C(\%t)$** |
|---|---|---|---|
| **57.10** | 63.14 | 0 | 0 |
| **47.67** | 36.21 | 0.01 | 1.769 |
| **42.61** | 21.75 | 0.08 | 14.15 |
| **39.80** | 13.71 | 0.16 | 28.31 |
| **39.47** | 12.78 | 0.24 | 42.47 |
| **38.61** | 10.32 | 0.32 | 56.63 |
| **38.48** | 9.964 | 0.4 | 70.79 |

Table 7. Hole expansion test results of IF steel.

| **Final average diameter $d_f$ (mm)** | **Hole expansion ratio $\lambda$ (%)** | **Cutting clearance $C$ (mm)** | **Cutting clearance in % of thickness $C(\%t)$** |
|---|---|---|---|
| **99.95** | 185.57 | 0 | 0 |
| **85.41** | 144.03 | 0.01 | 1.459 |
| **78.01** | 122.89 | 0.08 | 11.67 |
| **75.95** | 117.00 | 0.16 | 23.35 |
| **65.77** | 87.92 | 0.24 | 35.03 |
| **62.06** | 77.32 | 0.32 | 46.71 |
| **57.31** | 63.75 | 0.40 | 58.39 |

Figure 15 shows the hole expansion ratio $\lambda$ versus cutting clearance in terms of thickness (percentage) for the DP450 and IF steel. The hole

expansion ratio decreases with an increase in cutting clearance, irrespective of the material. In the case of the IF steel, the hole expansion ratio decreases almost linearly with an increase in the cutting clearance; however, the drop is slightly higher in the beginning. In the case of the DP450 steel, the drop in hole expansion with an increase in cutting clearance is significant at the beginning and very little after the initial drop. The hole expansion ratio's sensitivity to the cutting clearance is high at the beginning for the DP450 steel, and for the IF steel, it varies gradually throughout the band.

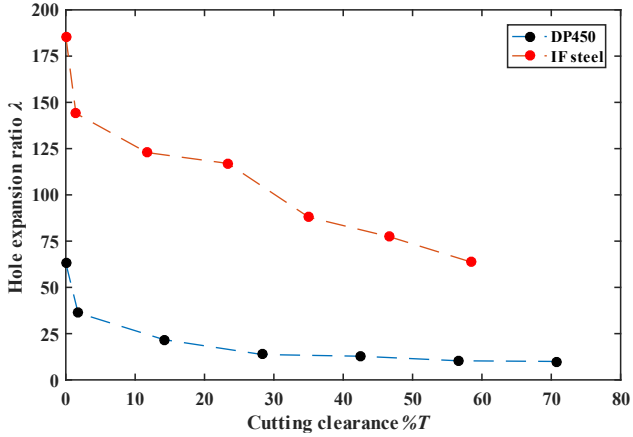


Figure 15. Hole expansion ratio λ versus cutting clearance for DP450 and IF steel.

## 8. CONCLUSION AND FUTURE WORK

Essential work of fracture (EWF) methodology has been studied, and parameters affecting the results are analysed in detail. The EWF method has been successfully used to calculate the fracture toughness of the DP450 steel and the IF steel. The EWF method can be used to characterise the strength and fracture toughness of advanced high-strength steels. This methodology helps in the selection of high-toughness and crash-resistant materials. However, the EWF methodology is sensitive to many parameters. The major parameters

affecting the EWF methodology are notch tip radius (fatigue pre-crack), sample preparation method, material property, selection of ligament length, choice of the lowest ligament length, and length of fatigue crack (*a/W* ratio). For the notched samples, the number of samples required to get accurate results is low (5 to 7). However, for precracked samples, a higher number of samples need to be tested for accurate results (more than 10). The sample preparation method influences the notch tip geometry and the results. However, for precracked samples, the influence of the sample preparation method is very low. The sample prepared from the EDM method is better than the laser cutting because it does not significantly change the material properties near the notch tip. However, the laser cutting produces a sharper notch tip, and the HAZ is offset by fatigue precrack. Both notched and precracked samples can be used in the EWF methodology. The notched samples are suitable for quick and easy comparison. However, only precracked samples represent the actual fracture toughness values. Low toughness and high strength materials like advanced high strength steels are more sensitive to notch tip radius. In contrast, high toughness materials are less sensitive to the notch tip radius. However, not all materials are equally sensitive to the notch tip radius.

Following conclusions can be made from the EWF tests, EBSD analyses, Fractographic analysis, FLD tests, hole expansion test of the IF steel and the DP450 steel.

- For the precracked samples, the DP450 and the IF steels have $w_e$ values of 154.22 kJ/m$^2$ and 196.16 kJ/m$^2$, respectively. The IF steel has about **27%** higher $w_e$ value than the DP450 steel.
- The presence of fatigue precrack in the DP450 steel has reduced $w_e$ by about 23%, while only 8% for the IF steel.

- For the precracked samples, crack tip-opening displacement $\delta_c^e$ for the DP450 and the IF steels are 0.3251 and 0.4260 mm, respectively. For the precracked samples, the IF steel has about **31%** higher $\delta_c^e$ value than the DP450 steel.
- For the precracked samples, $\psi^e$ for the DP450 and the IF steels are 9.07º and 19.76º, respectively.
- The average grain sizes are 6.31 µm and 15.35 µm for the DP450 and IF steels, respectively (considering only the grains larger than 100 pixels and without martensite for the DP450 steel).
- In the IF steel, a favourable {111} crystal orientation in the normal direction helps for excellent plastic deformation; however, the DP450 steel lack a favourable {111} texture in the normal direction.
- Both the DP450 steel and the IF steel have local misorientation in as-received condition. In the IF steel, local misorientation is concentrated mainly in small grains and around LAGB. In the DP450 steel, the local misorientation is primarily concentrated around martensite and grain boundaries.
- During plastic deformation, both the DP450 steel and the IF steel experience heterogeneous deformation within the ferrite grain. However, the extent of heterogeneous deformation is less in IF steel.
- Primary mode void generation in the DP450 steel is ferrite-martensite decohesion, and voids appeared in between two small martensite grains separated by a short distance. In the IF steel, voids formed only at grain boundary interactions.
- The size of the plastic zone during the EWF test is significantly larger for the IF steel than the DP450 steel (DIC analyses). The

IF steel can redistribute the stress much away from the crack tip.

- At zero clearance, the hole expansion ratio of the DP450 and the IF steels are 63.14 and 185.57 percentages respectively.
- In the FLD, for the near plane-strain condition, the IF steel has a major strain of **75.12%** higher than that of the DP450 steel.
- The IF steel has excellent necking characteristics, high elongation at fracture, good fracture toughness, better hole expansion ratio, and a favourable crystallographic orientation for better forming. The DP450 steel has decent fracture toughness, poor hole expansion ratio, poor necking characteristics, reasonable elongation at fracture, and high strength.
- In automotive body stamping, the IF steel has an edge in parts where the deep drawing (high-intensity forming) is necessary. However, the DP450 steel is still a good option for the parts, which do not require high-intensity forming but need high strength.

## REFERENCES


1. Fonstein, N. Dual-Phase Steels. In *Automotive Steels: Design, Metallurgy, Processing and Applications*; Elsevier Inc., 2016; pp 169–216. https://doi.org/10.1016/B978-0-08-100638-2.00007-9.
2. Ghosh, P.; Ray, R. K. Deep Drawable Steels. In *Automotive Steels: Design, Metallurgy, Processing and Applications*; Elsevier Inc., 2016; pp 113–143. https://doi.org/10.1016/B978-0-08-100638-2.00005-5.
3. Broberg, K. B. Critical Review of Some Theories in Fracture Mechanics. *International Journal of Fracture Mechanics* **1968**, *4* (1), 11–19. https://doi.org/10.1007/BF00189139.
4. M R, S. K.; Schmidova, E.; Konopík, P.; Melzer, D.; Bozkurt, F.; V Londe, N. Fracture Toughness Analysis of Automotive-Grade Dual-Phase Steel Using Essential Work of Fracture (EWF) Method. *Metals* **2020**, *10* (8), 1019. https://doi.org/10.3390/met10081019.
5. Cotterell, B.; Reddel, J. K. The Essential Work of Plane Stress Ductile Fracture. *International Journal of Fracture* **1977**, *13* (3), 267–277.

https://doi.org/10.1007/BF00040143.
6. Cotterell, B.; Pardoen, T.; Atkins, A. G. Measuring Toughness and the Cohesive Stress-Displacement Relationship by the Essential Work of Fracture Concept. *Engineering Fracture Mechanics* **2005**, *72* (6 SPEC. ISS.), 827–848. https://doi.org/10.1016/j.engfracmech.2004.10.002.
7. Hosford, W. F.; Atkins, A. G. On Fracture Toughness in Tearing of Sheet Metal. *Journal of Materials Shaping Technology* **1990**, *8* (2), 107–110. https://doi.org/10.1007/BF02833622.
8. Mai, Y.-W.; Cotterell, B. *On the Essential Work of Ductile Fracture in Polymers*; 1986; Vol. 32.
9. Frómeta, D.; Parareda, S.; Lara, A.; Molas, S.; Casellas, D.; Jonsén, P.; Calvo, J. Identification of Fracture Toughness Parameters to Understand the Fracture Resistance of Advanced High Strength Sheet Steels. *Engineering Fracture Mechanics* **2020**, *229*, 106949. https://doi.org/10.1016/j.engfracmech.2020.106949.
10. Clutton, E. Q. ESIS TC4 Experience with the Essential Work of Fracture Method. *European Structural Integrity Society* **2000**, *27* (C), 187–199. https://doi.org/10.1016/S1566-1369(00)80018-7.
11. Clutton, E. Essential Work of Fracture. *European Structural Integrity Society* **2001**, *28* (C), 177–195. https://doi.org/10.1016/S1566-1369(01)80033-9.
12. Atkins, A. G.; Mai, Y. W. Fracture Strains in Sheet Metalforming and Specific Essential Work of Fracture. *Engineering Fracture Mechanics* **1987**, *27* (3), 291–297. https://doi.org/10.1016/0013-7944(87)90147-0.
13. Frómeta, D.; Lara, A.; Grifé, L.; Dieudonné, T.; Dietsch, P.; Rehrl, J.; Suppan, C.; Casellas, D.; Calvo, J. Fracture Resistance of Advanced High-Strength Steel Sheets for Automotive Applications. *Metallurgical and Materials Transactions A: Physical Metallurgy and Materials Science* **2021**, *52* (2), 840–856. https://doi.org/10.1007/s11661-020-06119-y.
14. Frómeta, D.; Tedesco, M.; Calvo, J.; Lara, A.; Molas, S.; Casellas, D. Assessing Edge Cracking Resistance in AHSS Automotive Parts by the Essential Work of Fracture Methodology. *IOP Conf. Series: Journal of Physics: Conf. Series* **2017**, *896*, 12102. https://doi.org/10.1088/1742-6596/896/1/012102.
15. SONG, R.; PONGE, D.; RAABE, D. Influence of Mn Content on the Microstructure and Mechanical Properties of Ultrafine Grained C-Mn Steels. *ISIJ International* **2005**, *45* (11), 1721–1726. https://doi.org/10.2355/isijinternational.45.1721.
16. Sobotka, J.; Solfronk, P.; Kolnerová, M.; Zuzánek, L. UTILIZATION OF THE CONTACT-LESS OPTICAL SYSTEM FOR THE BORE EXPANSION TEST. In *22nd-International Conference on Metallurgy and Materials*; TANGER: Brno, 2013; pp 845–850.

17. Han, H.; Rollett, A.; Kim, D.; Oh, K. H.; Lebensohn, R. Subgrain Texture Evolution during Biaxial Deformation in Interstitial Free and Dual Phase Steels; 2009.
18. Deeparekha, N.; Gupta, A.; Demiral, M.; Khatirkar, R. K. Cold Rolling of an Interstitial Free (IF) Steel—Experiments and Simulations. *Mechanics of Materials* **2020**, *148*, 103420. https://doi.org/10.1016/j.mechmat.2020.103420.
19. Khatirkar, R.; Vadavadagi, B.; Haldar, A.; Samajdar, I. ND//<111> Recrystallization in Interstitial Free Steel: The Defining Role of Growth Inhibition. *ISIJ International* **2012**, *52* (5), 894–901. https://doi.org/10.2355/isijinternational.52.894.
20. Cruz-Gandarilla, F.; Salcedo-Garrido, A. M.; Bolmaro, R. E.; Baudin, T.; De Vincentis, N. S.; Avalos, M.; Cabañas-Moreno, J. G.; Mendoza-Leon, H. Microstructural Evolution and Mechanical Properties on an ARB Processed If Steel Studied by X-Ray Diffraction and EBSD. *Materials Characterization* **2016**, *118*, 332–339. https://doi.org/10.1016/j.matchar.2016.05.025.
21. Calcagnotto, M.; Adachi, Y.; Ponge, D.; Raabe, D. Deformation and Fracture Mechanisms in Fine- and Ultrafine-Grained Ferrite/Martensite Dual-Phase Steels and the Effect of Aging. *Acta Materialia* **2011**, *59* (2), 658–670. https://doi.org/10.1016/j.actamat.2010.10.002.